JACS
JOURNAL OF THE AMERICAN CHEMICAL SOCIETY

ARTICLE

pubs.acs.org/JACS

Transmission Coefficients for Chemical Reactions with Multiple States: Role of Quantum Decoherence

Aurélien de la Lande,[†,*] Jan Řezáč,[‡] Bernard Lévy,[†] Barry C. Sanders,[§] and Dennis R. Salahub[∥]

[†]Laboratoire de Chimie Physique—CNRS UMR 8000, Université Paris-Sud 11, Bât. 349, Campus d'Orsay, 15 rue Jean Perrin, 91 405 Orsay Cedex, France

[‡]Institute of Organic Chemistry and Biochemistry, Academy of Sciences of the Czech Republic and Center for Biomolecules and Complex Molecular Systems, Flemingovo nam. 2, 166 10 Prague 6, Czech Republic

[§]Institute for Quantum Information Science, University of Calgary, 2500 University Drive, Calgary, Canada T2N 1N4

[∥]Department of Chemistry, Institute for Biocomplexity and Informatics, and Institute for Sustainable Energy, Environment and Economy, University of Calgary, 2500 University Drive, Calgary, Canada T2N 1N4

ABSTRACT: Transition-state theory (TST) is a widely accepted paradigm for rationalizing the kinetics of chemical reactions involving one potential energy surface (PES). Multiple PES reaction rate constants can also be estimated within semiclassical approaches provided the hopping probability between the quantum states is taken into account when determining the transmission coefficient. In the Marcus theory of electron transfer, this hopping probability was historically calculated with models such as Landau−Zener theory. Although the hopping probability is intimately related to the question of the transition from the fully quantum to the semiclassical description, this issue is not adequately handled in physicochemical models commonly in use. In particular, quantum nuclear effects such as decoherence or dephasing are not present in the rate constant expressions. Retaining the convenient semiclassical picture, we include these effects through the introduction of a phenomenological quantum decoherence function. A simple modification to the usual TST rate constant expression is proposed: in addition to the electronic coupling, a characteristic decoherence time τ_{dec} now also appears as a key parameter of the rate constant. This new parameter captures the idea that molecular systems, although intrinsically obeying quantum mechanical laws, behave semiclassically after a finite but nonzero amount of time (τ_{dec}). This new degree of freedom allows a fresh look at the underlying physics of chemical reactions involving more than one quantum state. The ability of the proposed formula to describe the main physical lines of the phenomenon is confirmed by comparison with results obtained from density functional theory molecular dynamics simulations for a triplet to singlet transition within a copper dioxygen adduct relevant to the question of dioxygen activation by copper monooxygenases.

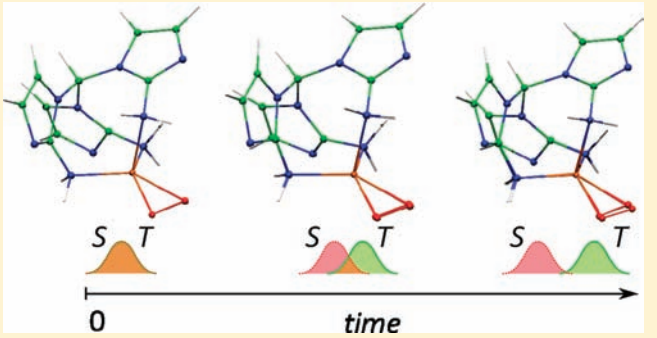

INTRODUCTION

Rationalizing the rates of chemical reactions in terms of simple and understandable concepts is one of the main objectives of theoretical chemistry. The establishment of reliable physicochemical models is, however, a challenging task owing to the complexity of the dynamics that underlies the molecular events and that is not necessarily amenable to reduction to a few-dimensional problem. In that regard, among the routes that have been followed to infer macroscopic kinetics laws from microscopic considerations, transition-state theory (TST) has certainly played a major role.[1−3] Indeed, most of our understanding of chemical reactivity rests on the intuitive view of nuclei moving on potential energy surfaces (PESs), traveling from the reactant valleys to the product valleys via the formation of activated complexes (transition states). Theories to deal with multiple-potential-energy-surface reactions have also been developed in the semiclassical limit. They can be related to TST through the concept of the transmission coefficient, which is a factor reflecting the probability of the quantum transition to occur at the TS.

The present approaches overlook one important property of such quantum systems, namely, the possibility of coherent superpositions of quantum states and the finite but nonzero time for which this superposition lasts. Inspired by the considerable literature devoted to the manifestation of decoherence in physicochemical processes,[4−10] we propose to employ the ideas developed by Neria et al.,[11] Prezhdo et al.,[4,5] and Jasper et al.[12] to follow the decoherence process. In this framework decoherence is modeled by a Gaussian or an exponential function of time with characteristic time τ_{dec}. This function corresponds to the decaying

Received: September 3, 2010
Published: February 23, 2011

overlap between nuclear wave packets evolving on different electronic states. We propose a modification of the semiclassical rate constant to introduce the characteristic decoherence time expression. This analytical, but approximate, formula is ultimately tested by comparison with density functional theory (DFT) numerical simulations, which estimate the transmission coefficient of a spin-crossing reaction for a copper dioxygen complex relevant to non-coupled copper monooxygenases.

TRANSITION-STATE THEORY

The rate constant of the chemical reaction is given by the rate of decomposition of the activated complex k_{TST}, assumed to be in equilibrium with the reactant:[13]

$$k_{TST} = [C_0]^{1-n} \nu \exp\left(-\frac{\Delta G^{\ddagger}}{RT}\right) \quad (1)$$

where $\Delta G^{\ddagger}$ is the Gibbs free energy of activation, ν is an effective frequency for the nuclear motion along the reaction coordinate (typically one takes $k_B T/h \approx 0.6 \times 10^{13}$ s^{-1} at 300 K), and n is the order of the reaction with respect to the standard-state reactant C_0. TST has been applied to quite different situations, in the gas phase as well as in condensed phases, for catalyzed or noncatalyzed chemical reactions. In particular, it appeared to be very helpful to establish the main lines of enzymatic catalysis, which is achieved mainly through the stabilization of the TS.[14] We do not review the enormous literature devoted to these topics, and the reader is referred instead to other papers for more information on TST.[3,15]

Commonly, the actual rate constant k is expressed as the product of k_{TST} with a transmission coefficient γ that accounts for the failure of certain conditions required for eq 1.[16] Following the terminology proposed by Garcia-Viloca et al.,[3,13] we decompose γ into three terms, Γ, g, and κ, which account respectively for the possibility of recrossings at the transition state, of nonequilibrium thermodynamic effects, and of quantum effects such as tunneling on the reaction coordinate:

$$k = \gamma k_{TST} = [C_0]^{1-n} \Gamma g \kappa \nu \exp\left(-\frac{\Delta G^{\ddagger}}{k_B T}\right) \quad (2)$$

The transmission coefficient γ provides a convenient way to relate the TST paradigm to other physicochemical models that were developed to describe chemical reactions involving more than one PES. Indeed, in many reactions the system must undergo hops between distinct quantum states before accessing the product valley. We may cite, nonexhaustively, electron transfers, spin-crossing reactions, electronic energy transfer, proton transfers, or proton-coupled electron transfers (PCETs). A possible strategy to obtain a semiclassical expression for the rate constant is to modify the transmission coefficient of the TST expression to account for the hopping probability between quantum states. Several formulas, such as the one derived in Landau−Zener−Stückelberg (LZS) theory, can be used to estimate such hopping probabilities.[17−19] The reader is referred to ref 20 or 21 for a review focusing on this type of approach in the context of spin-forbidden reactions. Alternatively, the Marcus theory of electron transfer is another example of a semiclassical framework which was developed to describe charge transfer reactions.[22−24] We also mention the strategy consisting of taking the semiclassical limit of the Fermi golden rule (FGR),[25] leading for instance to the nonadiabatic rate constant of Marcus theory (eq 3) or the Förster theory for electronic energy transfers.[26,27] In eq 3, H_{12} is the electronic coupling between the two quantum states and λ is the reorganization energy (see below). The Marcus theory now serves as a general semiclassical framework to describe various types of multiple PES reactions depending on the nature of the quantum states provided a perturbative treatment is reasonable. This is, for example, the case of some proton tunneling or PCET reactions.[28−32]

$$k_{ET} = \frac{2\pi}{\hbar} \frac{1}{\sqrt{4\pi\lambda k_B T}} |H_{12}|^2 \exp\left(\frac{-\Delta G^{\ddagger}}{k_B T}\right) \quad (3)$$

The above approaches have found compelling experimental corroboration. They allow one to express the rate constant of chemical processes involving multiple quantum states within a semiclassical framework. On the other hand, these theories cannot be considered as entirely satisfactory. Indeed various effects related to the quantum nature of atomic nuclei, such as nuclear interferences, are not, by definition, taken into account in such semiclassical pictures. Recent experimental findings challenge the adequacy of the semiclassical picture in certain types of reactions. This is, for instance, the case of exciton energy that is transferred coherently between chromophores of biological antennas or along conjugated polymers.[33−37] Another example is the case of long-range electron transfers that operate either through coherent (superexchange) or incoherent (electron-hopping) mechanisms. We finally note that some recent experimental studies show the possibility of modulating chemical rates by nuclear interferometry.[38,39]

These phenomena motivate an in-depth study of the requirements for a semiclassical picture to be adequate for the study of chemical reactivity. Actually, many studies have paved the way toward the introduction of nuclear quantum effects into physical chemistry problems.[4−9] Nevertheless, besides the necessary development of numerical approaches to simulate chemical events at the atomic scale, there is also the need to develop further simpler kinetic models to help interpret measured or computed rate constants in terms of accessible chemical theory. Here our objectives are, first, to develop an explicit intuitive picture of decoherence in the context of a chemical reaction and, second, to modify the Marcus equation to take into account decoherence with a simple characteristic parameter.

ESSENTIALS OF MARCUS THEORY

Time-Independent Picture. In this section we summarize the essentials of Marcus theory and stress the usual assumptions for estimating the transmission coefficient of these reactions. For simplicity, we discuss the two-state system (outlined in Figure 1, left side) and we will restrict our discussion to electron transfers. First, we define a basis representation for the quantum system. One choice is the adiabatic basis whose vectors $|\Psi_{\pm}\rangle$ are obtained as eigenvectors of the electronic Hamiltonian by resolution of the time-independent Schrödinger equation of the system for every fixed spatial configuration $\mathbf{R}$ of the nuclei. These eigenvectors correspond to eigenenergies $E_{\pm}$ and are coupled to each other through the dynamical coupling vector $d_{\pm} = \langle\Psi_{-}|\partial/\partial\mathbf{R}|\Psi_{+}\rangle$. Alternatively, the diabatic bases $\{|\phi_1\rangle, |\phi_2\rangle\}$, with eigenvalues $E_{1,2}$, are depicted in Figure 1 by solid curves. In the diabatic case the coupling between the two eigenstates takes the form $H_{12} = \langle\phi_1|H|\phi_2\rangle$, with H the electronic Hamiltonian.

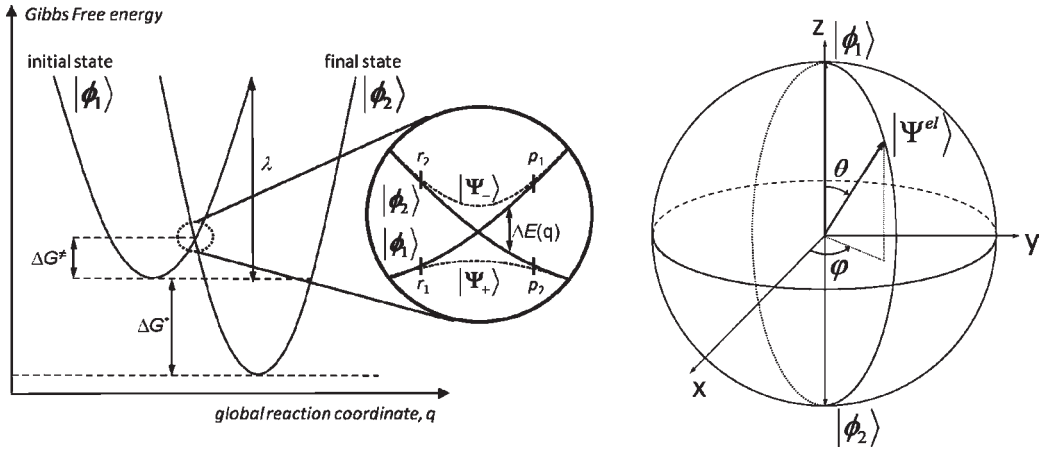

Figure 1. Two-level system in quantum mechanics. Left: Simplified energy profile along a one-dimensional global reaction coordinate q for a chemical reaction involving two PESs. The full lines represent the diabatic states, whereas the dashed lines are the adiabatic states (inset). At the crossing H_{12} is half the gap between E_- and E_+. λ is the reorganization energy, and ΔG° and $\Delta G^\ddagger$ are respectively the reaction Gibbs free energy and the Gibbs activation energy. The labels r_1, r_2, p_1, and p_2 in the inset symbolize the states in the system's configuration space depending on whether the system is in the reactant or product valley and in the first or second diabatic state. Right: Representation of the electronic state vector on the Bloch sphere. The angles θ and φ define the electronic state vector in the space spanned by the diabatic bases $\{|\phi_1\rangle, |\phi_2\rangle\}$.

The diabatic energy gap ($\Delta E = E_1 - E_2$) is the energy difference between the two diabatic states.

In principle, the diabatic vectors $|\phi_1\rangle$ and $|\phi_2\rangle$ are solutions of a time-independent Schrödinger equation for an unperturbed Hamiltonian H_0, i.e., the complete electronic Hamiltonian from which the coupling is removed. Although a rigorous definition of the unperturbed Hamiltonian is not possible in the general case,[40] there exist various technical procedures to approximate this Hamiltonian in practice (e.g., constrained DFT[41−43] or the valence bond method[44−46]). Various reasons motivate the use of the diabatic representation. For example, the diabatic representation may be easier to interpret in terms of chemical concepts than the adiabatic basis: in the case of electron transfer the diabatic basis corresponds to the electronic states for which the electron to be transferred is localized either on the oxidant or on the reductant (a similar description can apply for a proton transfer reaction). In addition, as illustrated in Figure 1, the diabatic eigenvectors are similar to their adiabatic counterparts when coupling strengths (either $d_\pm$ or H_{12}) tend to zero, that is, when the system is energetically far from the degeneracy region. Diabatic and adiabatic energies satisfy

$$E_\pm = \frac{1}{2}(E_1+E_2) \pm \frac{1}{2}\sqrt{\Delta E^2+|4H_{12}|^2} \qquad (4)$$

In Figure 1 we have adopted a one-dimensional parametrization with a global reaction coordinate q, recalling that, in real systems, q represents *all* atomic configurations required to bring the two quantum states into degeneracy. In complete coordinates (**R**), some degrees of freedom may not be coupled to the reaction; therefore, the transition state is not a single point in the multidimensional space, and following Lorquet et al., we use the term "seam region" to refer to all configurations for which $\Delta E \approx 0$ applies.[47] For practical purposes, we consider the energy difference ΔE itself as a meaningful global reaction coordinate.[41,45]

A reactive trajectory on the PES results from the combination of two successive events: first, thermal activation of the system whose probability is given by an exponential activation term and,

Scheme 1

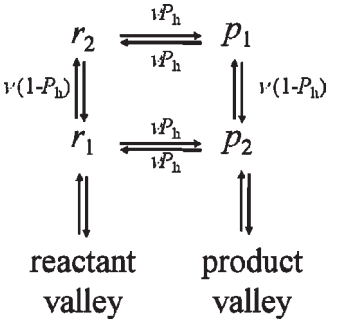

second, a quantum hop to the product state with hopping probability P_h. In the framework of eq 2, this event is quantified by the terms κ and Γ. For steady-state thermodynamics around the seam region, the transmission coefficient can be expressed from the effective frequency ν and the hopping probability P_h using the kinetics diagram in Scheme 1, where the notations $r_{1,2}$ and $p_{1,2}$ refer to the reactant (r) or product (p) valleys and states 1 and 2, as defined in Figure 1. The transmission coefficient can be written as $\gamma = g2\langle P_h\rangle/(1 + \langle P_h\rangle)$.[48] If one has to consider an ET reaction in the "inverted" region of Marcus theory, the kinetic scheme has to be modified slightly, and one finally obtains $\gamma = g2\langle P_h\rangle(1 - \langle P_h\rangle)$.[48]

Hopping Probabilities. Two limiting regimes are commonly defined according to the value of the hopping probability P_h. If $P_h \approx 1$, the reaction is said to be adiabatic. Each time the molecular system reaches the seam region, the probability to hop to the other quantum state is nearly 1. On the other hand, the hopping probability may be rather small ($P_h \ll 0.1$), and then the reaction is qualified as nonadiabatic. This nonadiabatic case is encountered in biological long-range ET,[49] in many spin-forbidden reactions, and in some proton-transfer reactions.[50,51] Traditionally, P_h has been estimated using the LZS formula relating P_h to the coupling between the quantum states and to the

dx.doi.org/10.1021/ja107950m |J. Am. Chem. Soc. 2011, 133, 3883–3894

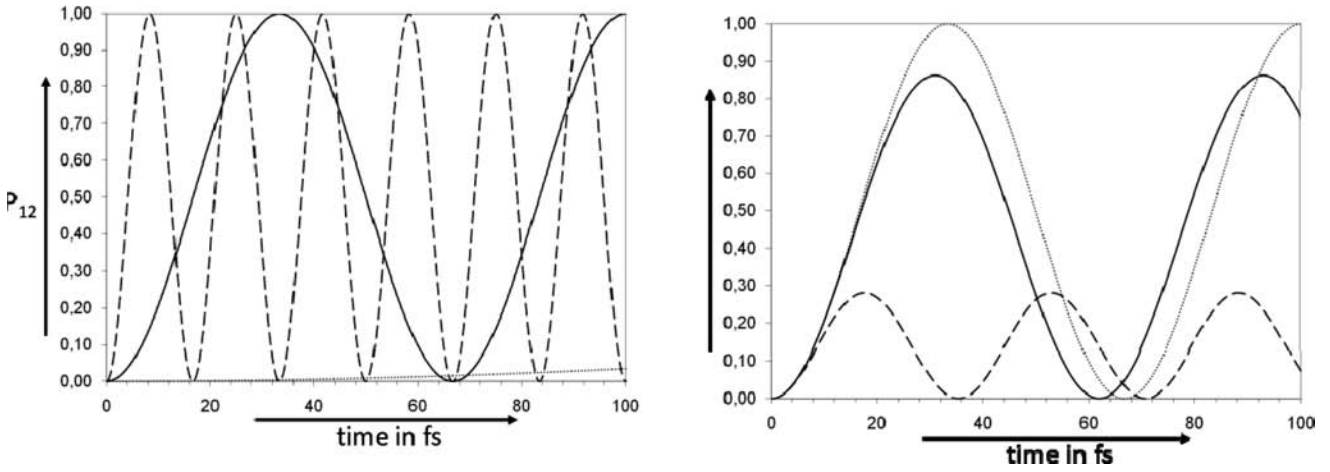

Figure 2. Coherent oscillations at different values of H_{12} and ΔE. Left: $\Delta E = 0$ cm^{-1} and $H_{12} = 10$ (dotted line), 200 (full line), or 1000 (dashed line) cm^{-1}. Right: $H_{12} = 200$ cm^{-1} and $\Delta E = 0$ (dotted line), 200 (full line), or 800 (dashed line) cm^{-1}.

sweeping rate, $|d\Delta E/dt|$, that is, the speed at which the system passes through the seam region:[17−19]

$$P_h^{LZ} = 1 - \exp\left[-2\pi {H_{12}}^2/\hbar \left|\frac{d\Delta E}{dt}\right|\right] \quad (5)$$

Sophisticated models have been proposed, for example, by Delos,[52] Demkov,[53] Bárany et al.,[54] and recently Zhu and Nakamura,[55−57] to correct inherent weaknesses of the LZS formula. However, these standard physical models do not take into account a point of fundamental importance, namely, the transition from the fully quantum to the semiclassical description. In this paper our objective is thus to include such aspects, building on the theory of decoherence.[58]

■ TRANSITION FROM THE QUANTUM TO THE SEMICLASSICAL PICTURE

Earlier we defined the quantum states $|\phi_1\rangle$ and $|\phi_2\rangle$ as being the solutions of the time-independent Schrödinger equation for the unperturbed Hamiltonian. The total electronic wave function $|\Psi^{el}(t)\rangle$ is a time-dependent linear combination of the states $|\phi_1\rangle$ and $|\phi_2\rangle$:

$$|\Psi^{el}(t)\rangle = c_1(t)|\phi_1\rangle + c_2(t)|\phi_2\rangle \quad (6)$$

$$i\hbar \frac{d}{dt}|\Psi^{el}\rangle = H|\Psi^{el}\rangle \quad (7)$$

Without loss of generality, the global phase of the state in eq 6 can be ignored so the two-level system can be parametrized by a polar angle θ and an azimuthal angle φ as

$$|\Psi^{el}(t)\rangle = \left(\cos\frac{\theta}{2}\right)|\phi_1\rangle + e^{i\varphi}\left(\sin\frac{\theta}{2}\right)|\phi_2\rangle \quad (8)$$

and depicted on the Bloch sphere (Figure 1, right). Here θ characterizes the weights of the basis vector, whereas φ represents the relative phase between these two eigenstates. Dynamically, the system undergoes coherent tunneling oscillations that result from the evolution in time of the coefficients c_1 and c_2 as a consequence of the Schrödinger equation (eq 7). Beginning with the initial conditions, $|\Psi^{el}(t=0)\rangle = |\phi_1\rangle(\theta=0°)$, the transition probability to measure the system in the second electronic state at a subsequent time t is given by projecting $|\Psi(t)\rangle$ onto $|\phi_2\rangle$ and taking the squared modulus of the resultant quantity:

$$P_{12}(t) = \frac{4|H_{12}|^2}{4|H_{12}|^2 + \Delta E^2} \sin^2\left[\sqrt{4|H_{12}|^2 + \Delta E^2}\,\frac{t}{2\hbar}\right] \quad (9)$$

Equation 9 is the well-known Rabi formula for the tunneling probability P_{12} as an oscillating function of time corresponding to angular frequency $\omega = (4{H_{12}}^2 + \Delta E^2)^{1/2}/\hbar$, which depends both on the electronic coupling and on the diabatic energy gap. Note that such an expression is only valid for constant H_{12} and ΔE. As illustrated in Figure 2, strong electronic coupling (e.g., 1000 cm^{-1}) induces rapid oscillations on the femtosecond time scale, whereas weak electronic coupling (<10 cm^{-1}) implies much slower oscillations (left panel of Figure 2). The right panel of Figure 2 illustrates, on the other hand, how the tunneling probability decays rapidly when the energy gap increases, although significant tunneling probabilities can be obtained with nonzero energy gaps. Now the question is how to relate the above two-state formalism to the transmission coefficient that enters the macroscopic rate constant.

The crucial observation is that, until a decoherence event occurs, the system remains in a coherent superposition of states. A completely decohering event would convert the state of the system into an incoherent mixture of states in some basis. To employ a semiclassical equation for the rate constant, such events certainly need to be taken into account when estimating the hopping probability. Standard hopping models, such as the one proposed by Zener, bypass this issue by making other hypotheses on the energy gap increase (and also on the electronic coupling term).[17]

For instance, to derive the LZS eq 5, ΔE is assumed to vary linearly with time, thereby becoming de facto the limiting parameter of the oscillations: when ΔE becomes large, the coefficients c_1 and c_2 are asymptotically constant, and the oscillation effectively ceases. The hopping probability is then taken as the limit of $P_{12}(t)$ when time tends to positive infinity. One may ask, for example, what will happen if the damping of the oscillation occurs on a shorter time scale, in particular while the system is still within the seam region? On the other hand, Onuchic and Wolynes showed clearly, for example, what may

be the impact of having successive recrossings while retaining quantum coherence between the electronic states.[59] They proposed an LZS-based expression for the final transmission coefficient taking into account such features, as well as the effect of interference among the nuclei on the hopping probability. We note that recent numerical simulations using a general harmonic oscillator model recently confirmed their predictions.[60] Zhao et al. compared the transmission coefficient as a function of a friction parameter that controls the number of recrossings, and factors of 2−7 were obtained for the hopping probability between the full quantum transmission coefficient and the hopping models commonly in use.[60] Their numerical study thus confirms the need to have a procedure that is able to provide at least reliable estimates of hopping probabilities taking into account explicitly the connections between the quantum and the semiclassical descriptions.

General Procedure: Theory of Quantum Decoherence. The physical systems we describe are comprised of light particles (the electrons) surrounding heavy atomic nuclei, both intrinsically obeying quantum mechanical laws. Our objective is to analyze under which conditions a semiclassical description can apply and to connect it to the full quantum description. So far the theoretical approaches have addressed this question through a perturbative treatment (e.g., the Fermi golden rule). Consequently, such frameworks cannot describe situations where the quantum nature of the nuclei plays more than just a perturbing role. Here we derive a new expression for the transmission coefficient that connects the quantum to the semiclassical description. The theory of decoherence is one path to modeling the quantum-to-classical transition by accounting for the progressive loss of coherence between two quantum states (here the electronic states) caused by interaction with the (classical) environment (the nuclei). Various experimental and theoretical studies have suggested that decoherence can be modeled as a decay function of time $D(t)$ with characteristic time τ_{dec}. Hence, we propose treating decoherence as a phenomenological parameter of the two-level dynamics. This changes the prevailing perspective where only the energy gap increase (or the electronic coupling variation) is the relevant parameter that determines the hopping probability to a novel view whereby the quantum-to-semiclassical transition dynamics is another central contributor to this probability.

In simple systems, two characteristic times are generally considered to account for decoherence. On one hand, τ_1 characterizes inelastic interactions of the quantum system with its environment (energy-increasing or energy-decreasing events such as energy dissipation that propel the system toward the ground state), whereas, on the other hand, τ_2 is the characteristic dephasing time (energy-conserving decohering events). The decoherence time τ_{dec} employed here accounts only for the first of these effects, within approximations discussed later. Pure dephasing between the electronic states (variations in the φ angle of the Bloch sphere) may arise from fluctuations in the energy gap due to elastic interaction with the environment (e.g., solvent). Such possibilities are not investigated here.

A related approach has been reported by Lockwood et al. within the context of the FGR and with connections to the semiclassical view. These authors applied this approach to ET within blue copper proteins.[61,62] Our approach is complementary to theirs in the sense that we stay close to the semiclassical picture, which has the advantage of being easier to comprehend. We also expect that the resulting semiclassical rate expressions have possible applications to problems that go beyond the perturbative domain. The scheme in Figure 3 outlines the main features of our approach for describing the quantum-to-semiclassical transition and the determination of the transmission coefficient γ.

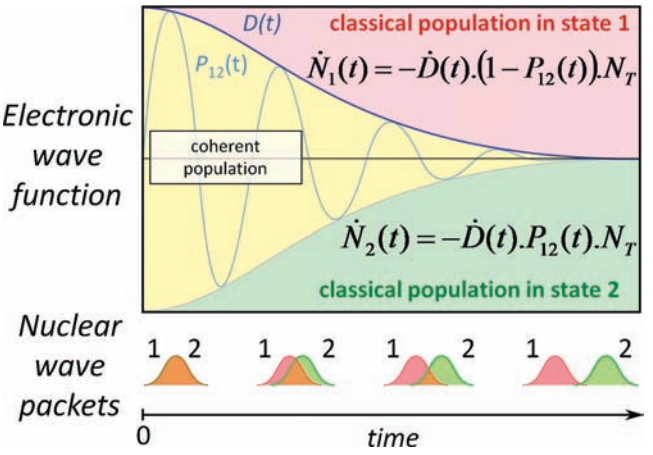

Figure 3. Schematic representation of the quantum-to-semiclassical transition and the accumulation over time of classical populations N_1 and N_2, respectively, in electronic states 1 and 2. For the sake of illustration, we have considered only a Gaussian function for $D(t)$ in this figure, but a similar picture would apply also for a first-order decay of the decoherence function.

The dynamics starts at $t = 0$ with a fully coherent initial state comprising N_T copies of the system under study and assumed to be in the seam region, defined by the condition $|\Delta E| < k_B T$. Since we work with the ensemble interpretation of quantum mechanics, it is redundant to involve copies of the investigated system. The N_T copies are mentioned here only for the sake of pedagogy. Interpreting the decaying decoherence function $D(t)$ as the fraction of this ensemble that remains in a superposition of states, the complementary function $1 - D(t)$ represents the fraction of the population that is either in state 1 or in state 2. At each time t, the coherent reservoir supplies the classical reservoirs depending on the actual value of $P_{12}(t)$. The final population N_2 of molecules in state 2 is thus obtained by integrating the classical kinetic law given in Figure 3, thus providing the final hopping probability to have reached state 2 once $D(t)$ has vanished, that is, when all the N_T replicate systems can be considered to behave as semiclassical again:

$$\langle P_h \rangle = -\int_0^{+\infty} P_{12}(t) \frac{dD(t)}{dt} dt \qquad (10)$$

Analytical Derivation of the Transmission Coefficient. As pointed out in the Introduction, the complexity of the dynamics of molecular systems necessitates some approximations if simple analytical formulas are desired. The accuracy of such approximations can then be tested with the help of numerical simulations (see the last section). To solve eq 10, one needs integrable expressions for $P_{12}(t)$ and $D(t)$. Different proposals for $D(t)$ have been made in the literature using either a first-order or a second-order form. Building on the work of Heller[63] and Neria et al.,[11,64] Prezhdo et al. proposed to model electronic decoherence by attributing the main cause to diminishing overlap of the nuclear wave function (Θ) with distinct electronic states.[4,5] This proposal is motivated by the fact that the off-diagonal elements of the density matrix are proportional to this overlap.[62] The

dx.doi.org/10.1021/ja107950m | J. Am. Chem. Soc. 2011, 133, 3883–3894

nuclear wave function is itself written as a product of the $3N - 6$ individual nuclear wave packets (NWPs). A global phase factor is also included for the NWP. The individual NWPs are described by frozen Gaussian functions (G_n):

$$|\Theta_\alpha\rangle = \prod_{n=1}^{3N-6} G_{\alpha n}(r, p, t) \exp\left[\frac{i}{\hbar}\int_0^\tau L_\alpha(\tau)\, d\tau\right] \quad (11)$$

$$G_{\alpha n}(r, p, t) = \left(\frac{a_n}{\pi}\right)^{3/4} \exp\left(-\frac{a_n}{2}(x - x_{\alpha n}(t))^2 + \frac{i}{\hbar}p_{\alpha n}(t)(x - x_{\alpha n}(t))\right) \quad (12)$$

where α refers to the electronic state, L_α is the Lagrangian, $a_n^{-1/2}$ is the wave packet width of the nth degree of freedom, and x and p are respectively the position and momentum of the nth degree of freedom. The overlap between the total nuclear wave functions evolving on distinct PESs thus involves both a phase factor (arising from the phase term) and an overlap term:

$$J(t) = \langle\Theta_1|\Theta_2\rangle = J_{\text{overlap}}(t)\, J_{\text{phase}}(t) \quad (13)$$

As an illustration, this scheme is depicted at the bottom of Figure 3 by showing two NWPs evolving on electronic states 1 and 2. This is a simplification as the true global overlap (eq 13) also involves the phase factor and the overlap in momentum space. At $t = 0$, the system is assumed to be in a coherent superposition, as reflected by an overlap of 1 of the nuclear wave function. However, the forces acting on the nuclei are not the same for the two electronic states, so the NWPs will necessarily diverge over time. The total overlap between the wave packets will thus decrease and decay to zero. In practice, because the total nuclear wave packet is a product of the individual atomic wave packets, the probability to return to a nonzero overlap at later times is negligible, and decoherence is effectively irreversible.

When the NWPs do not overlap anymore, the nuclear environment decoheres between electronic states 1 and 2. The probabilities are given respectively by the weights $|c_1|^2$ and $|c_2|^2$. In the context of the perturbative FGR, an exact meaning of the decoherence function could be given by Prezhdo et al.: $D(t)$ corrects the approximation that is made when going from the fully quantum FGR to a semiclassical one.[5] In the high-temperature limit, $D(t)$ takes the form of a Gaussian law (i.e., a second-order expression in time) characterized by a decoherence time τ_{dec}:

$$D(t) = \exp[-t^2/2\tau_{\text{dec}}^2] \quad (14)$$

Expression 14 is valid only for decoherence times short compared to the nuclear vibration period (∼tens of femtoseconds) and within the perturbative limit. These are actually the limits of applicability of the FGR. In the high-temperature limit, τ_{dec} can be estimated by the following expression:

$$\tau_{\text{dec}} = \left[\left\langle \sum_n \frac{1}{2a_n\hbar^2}(F_{1n} - F_{2n})^2 \right\rangle_T\right]^{-1/2} \quad (15)$$

F_{1n} and F_{2n} are the forces acting on the nth degree of freedom (the reader is referred to ref 5 for a full mathematical derivation). Physically, this equation reflects the fact that the atoms contributing the most to decoherence are those that feel different forces in the two electronic states. It is worth remarking that the set of atoms inducing decoherence are also those that are part of the global reaction coordinate as defined in semiclassical theories (e.g., Marcus theory).

More recently, Jasper and Truhlar proposed an alternative expression for $D(t)$.[12] These authors also follow the idea of monitoring decoherence by the decay of the overlap of the nuclear wave packets, but they use criteria formulated by Paz et al.:[65] "i) the semiclassical limit of a wave function is the sum of Wentzel-Kramers-Brillouin-like trajectories associated with minimum wave packets, and decoherence of the superposition is faster than decoherence of the individual packets (nuclear wave packets move at different speeds on different surfaces and get out of phase and out of overlap) and ii) ...the pointer basis is the one in which decoherence is the fastest".[66] They finally obtained a first-order expression:

$$D(t) = \exp[-t/\tau_{\text{dec}}] \quad (16)$$

Note that the characteristic decoherence time as defined in the work of Jasper and Truhlar is different from that proposed by Prezhdo et al. Now the expression for τ_{dec} contains two kinds of terms, one involving the difference in forces, $\tau_{\text{dec}}^{\Delta F}$, and one involving the difference in momentum, $\tau_{\text{dec}}^{\Delta p}$, between the nuclei of two electronic states:

$$\frac{1}{\tau_{\text{dec}}} = \frac{1}{\tau_{\text{dec}}^{\Delta F}} + \sqrt{\left(\frac{1}{\tau_{\text{dec}}^{\Delta p}}\right)^2 + \left(\frac{1}{\tau_{\text{dec}}^{\Delta F}}\right)^2} \quad (17)$$

$$\frac{1}{\tau_{\text{dec}}} = \sum_{n=1}^{3N-6} \frac{\pi}{2}\frac{F_{1n} - F_{2n}}{\bar{p}_n} + \sum_{n=1}^{3N-6}\sqrt{\left[\frac{(p_{1n} - p_{2n})^2|V_1 - V_2|}{4M_n\hbar^2\pi^2} + \frac{\pi^2}{4}\frac{(F_{1n} - F_{2n})^2}{\bar{p}_n^2}\right]} \quad (18)$$

$\bar{p}_n$ and M_n are respectively the average momentum and the mass of the nth nuclear degree of freedom. V_1 and V_2 are the potential energies on electronic states 1 and 2. To generalize the original equation of Jasper et al. to the multidimensional case, we have neglected the nuclear wave packet overlaps between different atoms. Although mathematically different, the characteristic decoherence times defined within the two approaches can be qualitatively related to one another if the momentum term in eq 17 vanishes. As remarked by Jasper et al., an encouraging point is to note that both approaches lead to decoherence times of similar order (ca. 1−50 fs), at least for the cases investigated so far. Actually, it is hard to tell which of the two expressions is the more correct due to the approximations that underlie their derivations, but the first-order expression is probably valid on longer time scales than the second-order one. Anyway, we will hereafter consider the two possibilities for the integration of eq 10: inserting eqs 9 and 14 (or 16) into eq 10, one obtains, after a few algebraic manipulations, the following hopping probabilities:

$$\text{first-order decay}: \quad D(t) = \exp[-t/\tau_{\text{dec}}]$$

$$\langle P_h\rangle \approx -\int_0^{+\infty} \sin^2\left(\frac{H_{12}t}{\hbar}\right)\frac{d}{dt}\left(\exp[-t/\tau_{\text{dec}}]\right) dt \quad (19a)$$

$$\langle P_h\rangle = \frac{4\mu^2}{\hbar^2 + 4\mu^2} \quad (19b)$$

$$\text{with} \quad \mu = H_{12}\tau_{\text{dec}} \quad (20)$$

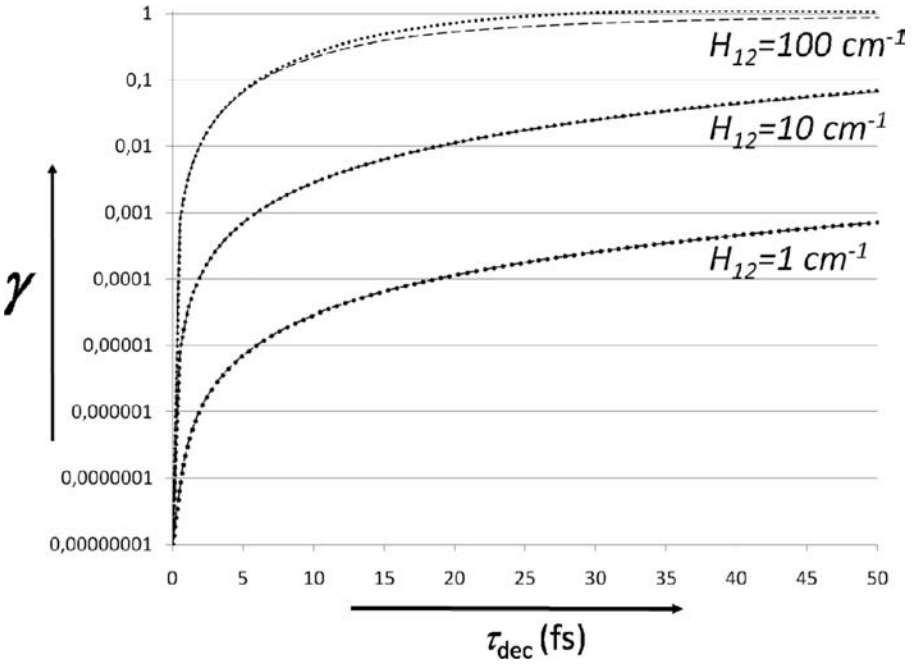

Figure 4. Transmission coefficient (logarithmic scale on the y axis) as a function of the characteristic decoherence time for various values of the electronic coupling. The dashed lines are the values obtained with the first-order decoherence function (eq 19b), while the dotted lines are obtained with the second-order formula (eq 21b with j = 21).

$$\text{second-order decay}: \quad D(t) = \exp[-t^2/2{\tau_{\text{dec}}}^2] \tag{19a}$$

$$\langle P_h\rangle \approx -\int_0^{+\infty} sin^2\left(\frac{H_{12}t}{\hbar}\right)\frac{d}{dt}\left(exp[-t^2/2{\tau_{\text{dec}}}^2]\right)dt \tag{21a}$$

$$\langle P_h\rangle = 4\left(\frac{\mu}{\hbar}\right)^2\sum_{j=1}^{\infty}\frac{1}{(2j-1)!!}\left(-8\frac{\mu^2}{\hbar^2}\right)^{j-1} \tag{21b}$$

$$\langle P_h\rangle = 4\left(\frac{\mu}{\hbar}\right)^2\left[1-\frac{8}{3}\frac{\mu^2}{\hbar^2}+\frac{64}{15}\frac{\mu^4}{\hbar^4}-\frac{512}{105}\frac{\mu^6}{\hbar^6}+\ldots\right] \tag{21c}$$

To obtain eqs 19a, 19b, 21a, 21b, and 21c, we assume (i) that the electronic coupling H_{12} remains constant in the seam region (the Condon approximation) and (ii) that the energy gap remains close to zero. Although this hypothesis may lead to an overestimate of the transition probability, it remains consistent with the use of TST or the Marcus formalism: the seam region is defined as the set of molecular configurations for which $\Delta E \approx 0$. This approximation will be tested in the last section.

Chemical Implications. In both eqs 19b and 21c, $\mu = H_{12}\tau_{\text{dec}}$ is the key parameter that controls the hopping probability, although through different expressions. The exponential-based expression for $\langle P_h\rangle$ presents a compact structure (eq 19b), while the Gaussian-based one presents a more complicated form involving an infinite sum of μ-dependent terms (eq 21c). Nonetheless, as illustrated in Figure 4, both formulas finally give very similar values, especially for short decoherence times or for weak electronic couplings. Since the exponential expression for $D(t)$ is expected to be valid on longer time scales, it appears to be more sensible to use eq 19b to calculate γ for all μ by $\gamma = g2\langle P_h\rangle/(1 + \langle P_h\rangle)$ (in the case of a reaction occurring in the normal region).[48] Using eq 19b and retaining the correction factor g that accounts for nonequilibrium effects, the rate constant (eq 2) is written as

$$k = [\text{C}_0]^{1-n}\nu g\frac{8\mu^2}{\hbar^2+8\mu^2}\exp\left(-\frac{\Delta G^{\ddagger}}{k_{\text{B}}T}\right) \tag{22}$$

1. Nonadiabatic Limit. When μ is small compared to $\hbar$ (short decoherence time or weak electronic coupling), eq 22 reduces to eq 23. Interestingly, we remark that the same expression is recovered from the second-order decoherence function if a first-order truncation of eq 21c is retained to estimate $\langle P_h\rangle$. It is thus apparent that in the nonadiabatic regime the shape of the function chosen for $D(t)$ does not have any significant influence on the rate constant expression. We can furthermore look for connections between the nonadiabatic limit of eq 22 and the nonadiabatic Marcus rate expression. To be consistent with our approach, we should compare eq 23 with a rate constant derived from eq 2 with a transmission coefficient estimated with the LZS formula (eq 5). This leads to eq 24. At this point it must be recalled that the notion of electronic decoherence is absent in the LZS framework, so eq 24 *does not* involve any decoherence time. We can however attempt to connect eqs 23 and 24 using the minimum-Heisenberg uncertainty relationship and approximating the sweeping rate ($|\text{d}\Delta E/\text{d}t|$) by $\hbar/{\tau_{\text{dec}}}^2$. The resulting eq 25 is then found to be close to our eq 23. In view of the different assumptions underlying the derivation of each of eqs 23 and 25, their similarity is encouraging.

$$k = [\text{C}_0]^{1-n}\nu g\frac{8\mu^2}{\hbar^2}\exp\left(-\frac{\Delta G^{\ddagger}}{k_{\text{B}}T}\right) \tag{23}$$

$$k = [\text{C}_0]^{1-n}\nu g\frac{4\pi {H_{12}}^2}{\hbar\left|\frac{\text{d}\Delta E}{\text{d}t}\right|}\exp\left(-\frac{\Delta G^{\ddagger}}{k_{\text{B}}T}\right) \tag{24}$$

dx.doi.org/10.1021/ja107950m |J. Am. Chem. Soc. 2011, 133, 3883–3894

$$k = [C_0]^{1-n} \nu g \frac{4\pi\mu^2}{\hbar^2} \exp\left(-\frac{\Delta G^{\ddagger}}{k_B T}\right) \quad (25)$$

2. Adiabatic Limit. We now focus on the opposite limit where $\mu \gg \hbar$. This is equivalent to considering the semiclassical limit ($\hbar \to 0$). Equation 22 now reduces to eq 26, which is in fact the adiabatic expression of Marcus theory where the transmission coefficient is close to unity.[26]

$$k = [C_0]^{1-n} \nu g \exp\left(-\frac{\Delta G^{\ddagger}}{k_B T}\right) \quad (26)$$

3. Influence of the Parameter τ_{dec}. As mentioned above, the time τ_{dec} is now a second independent parameter that enters the transmission factor in addition to H_{12}. This additional degree of freedom allows a fresh look at the underlying kinetics of these chemical reactions. Effectively, in conjunction with the electronic coupling, one can also modulate the rate constant by tuning τ_{dec}. Consider, for instance, a value of 100 cm^{-1} for H_{12}. As shown in the logarithmic plot of γ of Figure 4, a characteristic decoherence time of 1 fs leads to a transmission coefficient of 7×10^{-4}, but a time of 10 fs leads to a coefficient 100 times greater. Clearly, the time over which quantum coherences can be preserved in chemical systems has a direct and significant impact on the chemical rate constants. Therefore, the transition from the nonadiabatic to the adiabatic regimes is dependent not only on the value of H_{12} but also on τ_{dec}. In principle, an adiabatic regime is achievable even with moderate electronic coupling provided τ_{dec} is large enough. In that regard it is important to mention recent experimental findings that have revealed cases of electronic coherences persisting over tens or hundreds of femtoseconds.[33−37]

On the other hand, the loss of quantum coherence on a very short time scale leads to interesting consequences. Indeed, by studying the coherent oscillations in Figure 2 or even in eqs 19a, 19b, 21a, 21b, and 21c, for example, it is easily seen that, for fast decoherence (say below 0.1 fs), the hopping probability would be quite small. Consequently, the dynamics of the system would be slowed, and the hopping probability would be decreased (along with the rate constant). This effect, known as the quantum Zeno effect,[67] has been observed for various systems of physical interest but has not yet been investigated, to our knowledge, as an underlying effect on a chemical reaction.[68] At first glance one may attempt to decrease τ_{dec} for a chemical reaction by performing repetitive measurements of the quantum state of the system of interest (e.g., the redox state or the spin state). We moreover mention a discussion by O. Prezhdo on the relevance of the related quantum anti-Zeno effect in chemistry.[69] Experimental techniques operating on a short time scale, typically the femto- or attosecond time scale, would certainly be necessary to observe such effects. The possibility of these counterintuitive effects should, however, stimulate future experimental studies.

We conclude this section with a general comment on the physical meaning of the characteristic decoherence time appearing in eq 22. Molecules are composed of quantum particles and, as such, intrinsically obey quantum mechanical laws. However, after a finite time, molecules behave semiclassically, and the nuclear motions can be reasonably described by classical mechanics laws. In that regard, molecular systems can be regarded as mixed quantum classical systems for which dedicated conceptual frameworks combining quantum and classical mechanics in adequate proportions should be developed. The appearance of the characteristic time τ_{dec} in eq 22 reflects this idea in the context of chemical reactivity. Beyond the precise choice made for the shape of the decoherence function, the main result of the present paper is, in our opinion, to bring this important new dimension into the rational framework of chemical kinetics. An unprecedented rate constant expression that retains the intuitiveness of semiclassical theories while including some nuclear quantum effects in a nonperturbative way has been proposed.

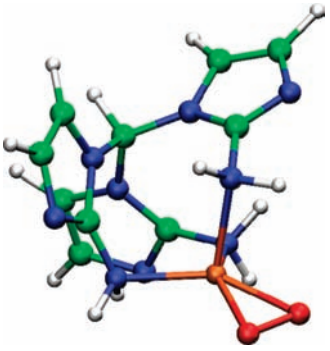

Figure 5. Copper dioxygen adduct mimicking the active site of noncoupled copper monooxygenases (oxygen in red, copper in orange, carbon in green, nitrogen in blue, and hydrogen in white).

NUMERICAL SIMULATIONS

In this section we employ a density-functional-theory-based approach to test the above theory and to compute the hopping probability for a spin-crossing reaction between a triplet (T) and a singlet (S) state within the copper dioxygen adduct depicted in Figure 5. This compound is a cuprous complex that represents a minimal model of the active sites of noncoupled copper monooxygenases.[70] In these enzymes the T to S transition is an essential step in the process allowing dioxygen activation, thus making it reactive toward aliphatic C−H bonds.[71] Many studies have been devoted to this class of chemical compounds, especially in terms of the relative stabilities of the two spin states.[72−75] However, few studies have attempted to describe the kinetics of this spin-forbidden reaction. The application of the formalism presented above to this particular reaction is thus also a good opportunity to investigate more deeply the question of dioxygen activation by mononuclear cuprous complexes.

Simulation Details. To obtain the average hopping probability $\langle P \rangle$ for the spin-crossing reaction from Born−Oppenheimer density functional theory molecular dynamics (BOMD), we employed the following two-step procedure. It has been applied to both the triplet-to-singlet transition and the reverse reaction. In the first step, we performed 13 and 8 ps of BOMD within the canonical ensemble (at T = 300 K) on either the triplet or the singlet surface (respectively for the T → S and the S → T reactions). The difference in simulation length was due to computational resource limitations. The DFT program deMon2k was used to perform all the DFT computations.[76] The Perdew−Becke−Ernzerhof (PBE) functional[77] was employed with a relativistic effective core potential (RECP) technique for the heavy atoms, while the double-ζ valence plus polarization functions (DZVP-GGA, generalized gradient

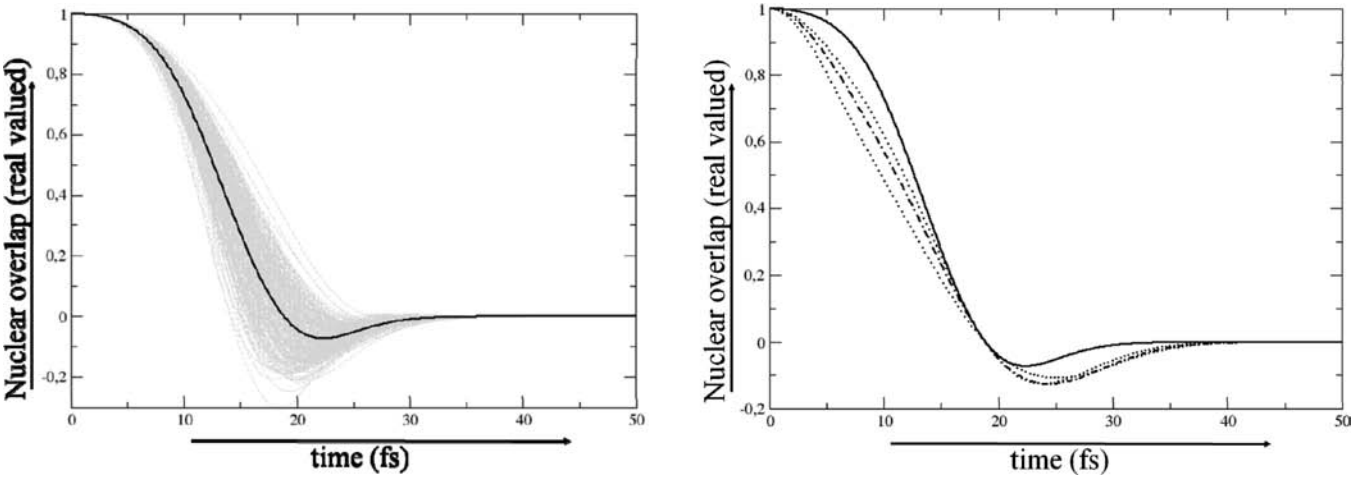

Figure 6. Real part of the nuclear overlap. Left: Averaged over 290 sets of diverging trajectories in gray (forward and backward reactions) using the high-temperature limit for a_n^{HT}. The black line is the average curve. Right: Effect of the frozen Gaussian widths on the average decoherence function. Key: full line, a_n^{HT}; dashed−dotted line, a_n^{MP2}; dotted lines, $a_n^{MP2} + \sigma_{a_n}^{MP2}$ (upper curve) and $a_n^{MP2} - \sigma_{a_n}^{MP2}$ (lower curve).

approximation) basis set was used for hydrogen atoms. A time step of 0.5 fs and a Nose−Hoover thermostat with a coupling frequency of 100 cm^{-1} were employed. In the TST picture the hopping probability reaches a maximum at the vicinity of the seam region. For this reason the MD simulations were biased to sample preferentially the seam region. To this end a biasing harmonic potential on the energy gap ΔE was applied:

$$V_{bias} = k_{bias}(\Delta E - 0)^2 = k_{bias}\Delta E^2 \qquad (27)$$

The force constant of the constraining potential k_{bias} was adjusted in preliminary tests to have an energy gap within $\pm k_B T$ around zero (in practice, at 300 K; a value of 1.76×10^3 kcal·mol^{-1}/(kcal·mol^{-1})^2 was used).

The initial trajectories were sampled at regular intervals (around 75 fs) to furnish the starting points for the second step of the procedure, namely, generation of the so-called diverging trajectories from which the hopping probability is evaluated with eq 10. More precisely, a set of diverging trajectories consists of two nonbiased BOMDs on the triplet and on the singlet surfaces along which decoherence is estimated by computing the overlap between the nuclear wave function on the T and S states. As this latter quantity depends on the kinetic energy of the nuclei, we switched to the microcanonical ensemble to avoid artifacts in the time evolution of the nuclear overlaps. We also decreased the time step to 0.1 fs when performing the diverging trajectories to improve the time resolution for the description of the decoherence process. As explained in the previous section, Gaussian wave packets are assigned to each degree of freedom of the molecule (three per atom, using Cartesian coordinates). As for any numerical method using Gaussian wave packets, a critical aspect is to specify the widths $a_n^{-1/2}$. To test the sensitivity of the computed decoherence times and hopping probabilities to these parameters, we have tested various alternatives for $a_n^{-1/2}$.

(a) The high-temperature values given by

$$a_n^{HT} = 6M_n k_B T/\hbar^2 \qquad (28)$$

where M_n is the atomic mass and T the temperature (300 K).[5,64]

(b) The ab initio parametrized values recently reported by Thompson et al. using second-order Møller−Plesset perturbative theory (MP2).[78] These authors adjusted the widths of the frozen Gaussian wave packets to reproduce the ground nuclear vibrational states which were obtained within the harmonic approximation. The fitting procedure was repeated for a large set of molecules. The authors provide both the average parameter a_n^{MP2} and its standard deviation ($\sigma_{a_n}^{MP2}$) for H, C, N, and O. The second term reflects the spread of the Gaussian widths among the set of molecules, i.e., the dependence of the widths on the chemical environment of the nuclei from one molecule to another. In our work we have thus tested three values: the average one (a_n^{MP2}) and the values $a_n^{MP2} \pm \sigma_{a_n}^{MP2}$. However, since no parameters have been reported for copper atoms in ref 78, we have kept the high-temperature value for this element. The boundary values for copper are taken to be $a_n^{HT} \pm 30\%$, which is roughly the standard deviation obtained for the atoms treated in ref 78.

Beyond the frozen Gaussian formalism, one could eventually allow the nuclear wave packets to breath over time due, for example, to population exchange. However, for the specific case investigated here, decoherence is found to occur rather quickly (in a few femtoseconds), and using time-dependent widths would give similar hopping probabilities and frozen Gaussian widths. Thus, we do not consider this alternative here.

While the NWP overlap is computed along 50 fs of the diverging trajectories, the coefficients $c_1(t)$ and $c_2(t)$ entering the expression of the total electronic wave function (eq 6) are evolved according to the time-dependent Schrödinger equation (eq 7). The initial values of the coefficients are estimated by a Boltzmann law using the initial diabatic energy gap. The subsequent evolution is performed numerically with a fourth-order Runge−Kutta algorithm,[79] using the diabatic energy gap extracted on-the-fly from the BOMD simulations and the electronic coupling, including the spin−orbit coupling terms, taken from ref 70 (H_{SO} = 85 cm^{-1}). In the present scheme electronic coupling is assumed to be constant during the simulation (Condon approximation). Equation 10 is integrated numerically over the ensemble of diverging trajectories to estimate the average transmission coefficients: around 180 sets were gathered for the forward reaction and around 110 sets for the backward reaction. As described in the following, rapid statistical convergence is reached when the number of sets of diverging trajectories is increased.

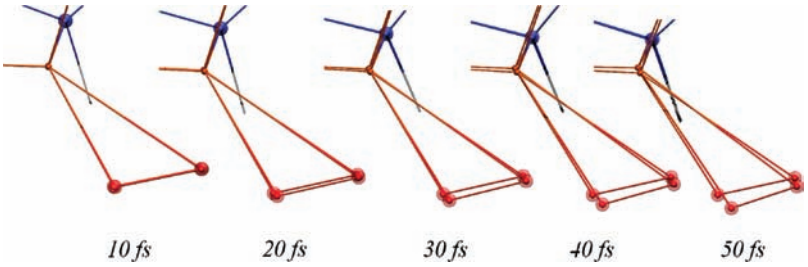

Figure 7. Divergence of the copper and oxygen nuclear wave packets and one nitrogen nuclear wave packet along the singlet and triplet trajectories (zoom on the CuO_2 core for one representative set). The transparent spheres represent the ab initio derived (N, O) or high-temperature (Cu) widths $a_n^{-1/2}$ of the nuclear wave packets (0.12 Å for N, 0.15 Å for O, and 0.02 Å for Cu).

Table 1. Characteristic Decoherence Times (fs) for Different Widths for the Nuclear Wave Packets[a]

	τ_{dec}^{init}	τ_{dec}^{div}			
width	a_n^{HT}	a_n^{HT}	a_n^{MP2}	$a_n^{MP2}+\sigma_{a_n}^{MP2}$	$a_n^{MP2}-\sigma_{a_n}^{MP2}$
T → S	12.2	11.7	9.7	10.5	8.3
S → T	8.2	11.3	9.2	10.0	7.9

[a] The temperature chosen to calculate a_n^{HT} is 300 K.

Table 2. Hopping Probabilities for the Forward and Backward Spin-Crossing Reactions within the Copper Dioxygen Adduct[a]

			$\langle P_{an}^{HT}\rangle$			$\langle P_{num}^{HT}\rangle$	
		$\langle P_{LZ}\rangle$	eq 19b	eq 21b (j = 1)	eq 21b (j = 70)	av	SD
T → S	a_n^{HT}	0.401	0.123	0.140	0.128	0.046	0.005
	a_n^{MP2}		0.088	0.096	0.091	0.035	0.004
S → T	a_n^{HT}	0.397	0.116	0.131	0.120	0.047	0.005
	a_n^{MP2}		0.080	0.087	0.082	0.036	0.004

[a] The hopping probabilities calculated numerically from the MD simulations ($\langle P_{num}^{HT}\rangle$) are the least approximate results and should serve as a reference.

Results. Figure 6 provides a picture of the loss of overlap between the NWPs for the 290 sets of diverging trajectories, and Figure 7 provides a molecular picture of the process for 1 set of diverging trajectories. We note that decoherence arises mainly from the diverging motion of the copper and oxygen atoms, consistent with the molecular orbital (MO) diagram of these systems: the singlet and triplet states differ mainly by the occupation of the bonding and antibonding MOs that involve copper d orbitals and the dioxygen π^* MO.[80] We note that other atoms coordinating the copper (three nitrogens) only have a minor contribution to the decoherence. We now look at the average curve $\langle D(t)\rangle$. Its evolution is close to a Gaussian shape that tends to zero after a few tens of femtoseconds, whatever the choice made for the widths. Such a Gaussian behavior is not surprising since in the present case the electronic coherences are lost rapidly and a second-order decay was expected. The characteristic decoherence times for the forward and backward reactions τ_{dec}^{div}, estimated from the average diverging trajectories, amount to 11.5 fs with the high-temperature widths and to ca. 9.5 fs with the ab initio derived widths (Table 1). These values are qualitatively similar and are close to those reported by other groups for systems of physical-chemical interest.[81] We however remark that this study, performed in vacuo, may underestimate both inelastic (τ_1) and elastic (τ_2) interactions between the solute and the environment (mainly the solvent) and consequently may overestimate the actual decoherence times observed in solution. An obvious computational protocol would be to use hybrid QM/MM (quantum mechanics/molecular mechanics) schemes to include the environment explicitly in the simulations. Such work is under way and will be reported in due course.

In the short time limit the characteristic decoherence time can also be estimated solely from the initial trajectories without carrying out the computationally intensive, diverging BOMD simulations. Prezhdo et al.[5] proposed to evaluate the characteristic decoherence time from the difference in forces from two PESs acting on the degrees of freedom n. As already mentioned, by using a Taylor expansion of the nuclear wave function overlap truncated at the second order, the high-temperature decoherence time can be estimated by eq 15. For the molecular system investigated here the distribution of τ_{dec}^{init} over the initial dynamics is substantially more spread out than the τ_{dec}^{div} distribution obtained from the diverging trajectories. This may come from the truncation order used in eq 15. However, both these distributions have a maximum at similar time τ, and the maximum value of τ_{dec}^{init} is found to be really close to that of τ_{dec}^{div}. If the same relationship were observed in other systems, it would be possible to develop a procedure for estimating more accurate τ_{dec} from the maximum of the distribution of τ_{dec}^{init} by reconstructing a narrower distribution mimicking that of τ_{dec}^{div}. For now, we recommend the evaluation of the average decoherence time from the simulation of diverging trajectories.

We now focus on the estimation of the hopping probability by the expressions proposed in the previous section. The estimates for $\langle P_h\rangle$ obtained by various formulas are reported in Table 2, all making use of the Condon approximation. $\langle P_{LZ}\rangle$ is obtained from the Landau−Zener−Stückelberg formula given by eq 5. To use this expression, the sweeping rate was estimated by taking the average value of $|d\Delta E/dt|$ over the first 1/2 fs of each set of diverging trajectories. $\langle P_{an}\rangle$ is the hopping probability calculated with the analytical formulas (eq 19b or 21c) using the characteristic decoherence time τ_{dec}^{div}. $\langle P_{num}\rangle$ is finally obtained by numerical evaluation of eq 10. We note that the simulation protocol employed here does not take into account the coherent evolution of the coefficients while the system approaches the seam region. However, in the present case, because decoherence is found to be faster than the time it takes for the system to lose (or gain) k_BT of energy, this possibility should be negligible.

The values obtained by the latter approach are close to 0.04, whatever the direction of the chemical reaction. We also note that

the distribution of the hopping probability over the sets of diverging trajectories is rather peaked around the average value as testified by the very small standard deviation (around 0.005). In the reaction investigated here, it is adequate to uncouple the thermal activation part from the quantum hopping part by the use of eqs 2 and 22. The choice of values of the widths does not have a strong effect on the hopping probabilities obtained numerically nor on the standard deviations. The comparison between the numerical and analytical estimations $\langle P_{an}^{HT} \rangle$ and $\langle P_{num}^{HT} \rangle$ is encouraging even though the analytical expressions slightly overestimate the hopping probabilities. This is due to the approximations made in the analytical integration of eq 10, namely, the assumption of a constant and null energy gap and the pure Gaussian form for $D(t)$. This overestimation is nevertheless reduced when using the a_n^{MP2} values since they are smaller than the a_n^{HT} values. The analytical expression should be all the more valid when the decoherence time is short compared to the time required for the system to drift away from the null energy gap region. As mentioned above, the explicit inclusion of the environment in the simulation, for instance, with hybrid QM/MM, would certainly help in reducing the differences between $\langle P_{an}^{HT} \rangle$ and $\langle P_{num}^{HT} \rangle$ by inclusion of solvent-induced decoherence.

The values provided by the various analytical expressions (eqs 19b and 21b) are found to be close to each other. Following our analysis of the previous section, this is the case because both the electronic coupling and the characteristic decoherence times are small. In such cases it was shown that both the first-order and second-order $D(t)$ give similar hopping probabilities in the nonadiabatic regime and that a first-order truncation of eq 21b was also enough. The numerical results thus fully support the analytical prediction. In both the forward and backward reactions, we note that the LZS formula predicts transmission coefficients higher than those predicted by the decoherence-based approach by about an order of magnitude.

CONCLUSION

In this paper, we have derived a simple analytical formula that allows the inclusion of quantum-mechanical effects in chemical reactions involving two PESs using a semiclassical approach. Inspired by various previous work,[4,5,61,62,81] we have treated quantum decoherence as a phenomenological parameter, and we have obtained a correction to the usual Marcus expression.

To test our analytical formula, we compared it to numerical simulations based on Born−Oppenheimer molecular dynamics using density functional theory. These simulations are the first application of this procedure to a spin-crossing reaction. The results for our model system mimicking the active site of a copper monooxygenase show encouraging agreement between analytical solution and results obtained from the simulation, with significant improvements over the LZS formula.

The rate constant appears to be a quadratic function of the electronic coupling (as in the usual theory) and of the characteristic decoherence time (the single new parameter added) that accounts for dissipation of energy to the nuclei. The proposed formula (eq 22) reduces to the nonadiabatic or the adiabatic expressions of Marcus theory depending on the values of the electronic coupling and of the characteristic decoherence time. Equation 22 moreover bridges the gap between these limit regimes. Pure dephasing effects that can also lead to decoherence will have to be included in future work.

The previous approaches, such as the LZS formula, had been derived from limit regimes in which quantum coherences are instantaneously destroyed or persevere indefinitely. The appearance of the characteristic decoherence time in eq 22 reflects the fact that quantum superposition of electronic states can last for finite but nonzero times and as such eq 22 can be regarded as a mixed quantum classical rate constant expression. Due to its simplicity, eq 22 should be useful to discuss decoherence effects on the basis of experimental data, for example, in enzymology. We also draw attention to the fact that, beyond the case of electron transfer or spin-crossing reactions treated here, the present formalism may also apply to other types of chemical reactions where the quantum states of interest are not of an electronic nature, as in the case of proton tunneling.

We conclude by noting that, in evolution-engineered systems such as enzymes, it would be worth examining whether some nuclear vibrations induce decoherence in synchrony with coherent tunneling oscillations. Depending on the amplitude of these effects on chemical rate constants, they could be important elements to include in our understanding of enzymatic catalysis of nonadiabatic chemical reactions. Wolynes recently used the picture of (decohering) clocks to name this hypothetical phenomenon: "if ... the heavy atoms repetitively carry out nearly the same motion like a clock, while the quantum choices are being made, the phases of the paths will add in some consistent fashion, perhaps destructively or perhaps constructively".[82] The present work provides a good starting point for future analytical *and* numerical developments.

AUTHOR INFORMATION

Corresponding Author
aurelien.de-la-lande@u-psud.fr

ACKNOWLEDGMENT

We thank Prof. I. Demachy, Dr. J. Ridard, and N. Babcock for helpful discussions. Ongoing support from NSERC, iCORE, and AIF is gratefully acknowledged. We are grateful to Compute Canada/WestGrid for computational resources. B.C.S. is a CIFAR Fellow.

REFERENCES

(1) Jortner, J. *J. Chem. Phys.* **1974**, *64*, 4860.
(2) Vanden-Eijnden, E.; Tal, A. J. *Chem. Phys.* **2005**, *123*, 184103.
(3) Truhlar, D. G.; Garrett, B. C.; Klippsenstein, S. J. *J. Phys. Chem.* **1996**, *100*, 12771 and references therein.
(4) Schawrtz, P. J.; Bittner, E. R.; Prezhdo, O. V.; Rossky, P. J. *J. Chem. Phys.* **1996**, *104*, 5942.
(5) Prezhdo, O. V.; Rossky, P. J. *J. Chem. Phys.* **1997**, *107*, 5863.
(6) Zhu, C.; Jasper, A.; Truhlar, D. G. *J. Chem. Theory Comput.* **2005**, *1*, 527.
(7) Kapral, R. *Annu. Rev. Phys. Chem.* **2006**, *57*, 129.
(8) Grunwald, R. B.; Kim, H.; Kapral, R. *J. Chem. Phys.* **2008**, *128*, 164110.
(9) Granucci, G.; Persico, M. *J. Chem. Phys.* **2007**, *126*, 134114.
(10) Drukker, K. *J. Comput. Phys.* **1999**, *153*, 225.
(11) Neria, E.; Nitzan, A. *Chem. Phys.* **1994**, *183*, 351.
(12) Jasper, A.; Truhlar, D. G. *J. Chem. Phys.* **2005**, *123*, 064103.
(13) Garcia-Viloca, M.; Gao, J.; Karplus, M.; Truhlar, D. G. *Science* **2004**, *303*, 186.
(14) Olsson, M. H. M.; Mavri, J.; Warshel, A. *Philos. Trans. R. Soc. London, B* **2006**, *361*, 1417.
(15) Hänggi, P.; Talkner, P.; Borkovec, M. *Rev. Mod. Phys.* **1990**, *62*, 251.
(16) Wigner, E. *Trans. Faraday Soc.* **1938**, *3*, 7.

(17) Zener, C. *Proc. R. Soc. London* **1932**, *137*, 696.
(18) Landau, L. D. *Phys. Z. Sowjetunion* **1932**, *2*, 46.
(19) Stückelberg, E. C. G. *Helv. Phys. Acta* **1932**, *5*, 396.
(20) Zahr, G. E.; Preston, R. K.; Miller, W. H. *J. Chem. Phys.* **1975**, *62*, 1127.
(21) Harvey, J. N. *Phys. Chem. Chem. Phys.* **2007**, *9*, 331 and references therein.
(22) Newton, M. D.; Sutin, N. *Annu. Rev. Phys. Chem.* **1984**, *35*, 437.
(23) Marcus, R. A. *J. Chem. Phys.* **1962**, *20*, 359.
(24) Marcus, R. A. *J. Chem. Phys.* **1965**, *43*, 2658.
(25) Miyashita, O.; Okamura, M. Y.; Onuchic, J. N. *J. Phys. Chem. B* **2003**, *107*, 1230.
(26) Marcus, R. A.; Sutin, N. *Biochim. Biophys. Acta* **1985**, *811*, 265.
(27) See for instance: *Phys. Chem. Chem. Phys.* **2010**, *12*, 7317 (special issue introduced by A. Harriman).
(28) Marcus, R. A. *J. Chem. Phys.* **2006**, *125*, 194504.
(29) Nagel, Z. D.; Klinman, J. P. *Chem. Rev.* **2006**, *106*, 3095.
(30) Nagel, Z. D.; Klinman, J. P. *Nat. Chem. Biol.* **2009**, *5*, 543.
(31) Truhlar, D. G. *J. Phys. Org. Chem.* **2010**, *23*, 660.
(32) Hammes-Schiffer, S. *Acc. Chem. Res.* **2009**, *42*, 1881.
(33) Lee, H.; Cheng, H.-C.; Fleming, G. R. *Science* **2007**, *316*, 1462.
(34) Collini, E.; Wong, C. Y.; Wilk, K. E.; Curmi, P. M.; Brumer, P.; Scholes, G. D. *Nature* **2010**, *463*, 664.
(35) Collini, E.; Scholes, G. D. *Science* **2009**, *263*, 369.
(36) Ishizaki, A.; Calhoun, T. R.; Schlau-Cohen, G. S.; Fleming, G. R. *Phys. Chem. Chem. Phys.* **2010**, *12*, 7319.
(37) Davis, A.; Cannon, E.; Van Dao, L.; Hannaford, P.; Quiney, H. M.; Nugen, K. A. *New J. Phys.* **2010**, *12*, 085015.
(38) Xiao, D.; Skourtis, S. S.; Rubtsov, I. V.; Beratan, D. N. *Nano Lett.* **2009**, *9*, 1818.
(39) Lin, Z.; Lawrence, C. M.; Xiao, D.; Kireev, V. V.; Skourtis, S. S.; Sessler, J. L.; Beratan, D. N.; Rubtsov, I. V. *J. Am. Chem. Soc.* **2009**, *131*, 18060.
(40) Mead, C. A.; Truhlar, D. G. *J. Chem. Phys.* **1982**, *77*, 6090.
(41) Hong, G.; Rosta, E.; Warshel, A. *J. Phys. Chem. B* **2006**, *110*, 19570.
(42) Wu, Q.; Van Voorhis, T. *Phys. Rev. A* **2005**, *72*, 024502.
(43) de la Lande, A.; Salahub, D. R. *J. Mol. Struct.: THEOCHEM* **2010**, *943*, 115.
(44) Hiberty, P. C.; Shaik, S. *J. Comput. Chem.* **2007**, *28*, 137.
(45) Kamerlin, S. C. L.; Cao, J.; Rosta, E.; Warshel, A. *J. Phys. Chem. B* **2009**, *113*, 10905.
(46) Valero, R.; Song, L.; Gao, J.; Truhlar, D. G. *J. Chem. Theory Comput.* **2009**, *5*, 1.
(47) Lorquet, J. C.; Leyh-Nihant, B. *J. Phys. Chem.* **1988**, *92*, 4778.
(48) Newton, M. D.; Sutin, N. *Annu. Rev. Phys. Chem.* **1984**, *35*, 437.
(49) Gray, H. B.; Winkler, J. R. *Q. Rev. Biophys.* **2003**, *36*, 341.
(50) Sutcliffe, M. J.; Masgrau, L.; Roujeinikova, A.; Johannissen, L. O.; Hothi, P.; Basran, J.; Ranaghan, K. E.; Mulholland, A. J.; Leys, D.; Scrutton, N. S. *Philos. Trans. R. Soc. London, B* **2006**, *361*, 1375.
(51) Alleman, R. K.; Scrutton, N. S. *Quantum Tunnelling in Enzyme-Catalysed Reactions*; Springer: New York, 2009.
(52) Delos, J. B. *J. Chem. Phys.* **1973**, *59*, 2365.
(53) Demkov, Y. N. *Sov. Phys. JETP* **1964**, *18*, 138.
(54) Bárány, A.; Crothers, D. S. F. *Proc. R. Soc. London, A* **1983**, *385*, 129.
(55) Nakamura, H. *J. Theor. Comput. Chem.* **2005**, *4*, 127.
(56) Zhu, C. *Phys. Scr.* **2009**, *80*, 048114.
(57) Nakamura, H. *J. Phys. Chem. A* **2006**, *110*, 10929.
(58) Zurek, W. H. *Los Alamos Sci.* **2002**, *No. 27*, arXiv:quant-ph/0306072v1.
(59) Onuchic, J. N.; Wolynes, P. G. *J. Phys. Chem.* **1988**, *92*, 6495.
(60) Zhao, Y.; Li, X.; Zheng, Z.; Liang, W. *J. Chem. Phys.* **2006**, *124*, 114508.
(61) Lockwood, D. M.; Cheng, Y. -K.; Rossky, P. J. *Chem. Phys. Lett.* **2001**, *345*, 159.
(62) Lockwood, D. M.; Hwang, H.; Rossky, P. J. *Chem. Phys.* **2001**, *268*, 285.
(63) Heller, E. J. *J. Chem. Phys.* **1981**, *75*, 2923.
(64) Neria, E.; Nitzan, A. *J. Chem. Phys.* **1993**, *99*, 1109.
(65) Paz, J. P.; Habib, S.; Zurek, W. H. *Phys. Rev. D* **1993**, *47*, 488.
(66) Cheng, S. C.; Zhu, C.; Liang, K. K.; Lin, S. H.; Truhlar, D. G. *J. Chem. Phys.* **2008**, *129*, 024112.
(67) Misra, B.; Sudarshan, E. C. G. *J. Math. Phys.* **1977**, *18*, 756.
(68) Bernu, J.; Deléglise, S.; Sayrin, C.; Kuhr, S.; Dotsenko, I.; Brune, M.; Raimond, J. M.; Haroche, S. *Phys. Rev. Lett.* **2008**, *101*, 180402.
(69) Prezhdo, O. V. *Phys. Rev. Lett.* **2000**, *85*, 4413.
(70) de la Lande, A.; Salahub, D.; Moliner, V.; Gérard, H.; Piquemal, J.-P.; Parisel, O. *Inorg. Chem.* **2009**, *48*, 7003.
(71) de la Lande, A.; Parisel, O.; Moliner, V.; Gérard, H.; Reinaud, O. *Chem.—Eur. J.* **2008**, *14*, 6465.
(72) Cramer, C J.; Gour, J. R.; Kinal, A.; Włoch, M.; Piecuch, P.; Shahi, A. R. M.; Gagliardi, L. *J. Phys. Chem. A* **2008**, *112*, 3754.
(73) Cramer, C. J.; Tolman, W. B. *Acc. Chem. Res.* **2007**, *40*, 601.
(74) de la Lande, A.; Salahub, D. R.; Maddaluno, J.; Scemama, A.; Pilme, J.; Parisel, O.; Gérard, H.; Caffarel, M.; Piquemal, J.-P. *J. Comput. Chem.* **2010**, in press, DOI: 10.1002/jcc.21698.
(75) de la Lande, A.; Moliner, V.; Parisel, O. *J. Chem. Phys.* **2007**, *126*, 035102.
(76) deMon2k: A. M. Köster, P. Calaminici, M. E. Casida, R. Flores-Moreno, G. Geudtner, A. Goursot, Th. Heine, A. Ipatov, F. Janetzko, J. M. del Campo, S. Patchkovskii, J. Ulises Reveles, D. R. Salahub, A. Vela, deMon Developers, 2006.
(77) Perdew, J. P.; Burke, K.; Ernzerhof, M. *Phys. Rev. Lett.* **1996**, *77*, 3865.
(78) Thompson, A. L.; Punwong, C.; Martínez, T. J. *Chem. Phys.* **2010**, *370*, 70.
(79) Press, W. H.; Teukolsky, S. A.; Vetterling, W. T.; Flannery, B. P. *Numerical Recipes*; Cambridge University Press: Cambridge, U.K., 1992.
(80) de la Lande, A.; Gérard, H.; Moliner, V.; Izzet, G.; Reinaud, O.; Parisel, O. *J. Biol. Inorg. Chem.* **2006**, *11*, 593.
(81) Turi, L.; Rossky, P. J. *J. Chem. Phys.* **2004**, *120*, 3688.
(82) Wolynes, P. G. *Proc. Natl. Acad. Sci. U.S.A.* **2009**, *106*, 17247.